

Direct torque control improvement for PMSM drive based on FLC

A. E. Rabhi^{1,*}, K. Hartani², Y. Guettaf¹

¹ Laboratory of Instrumentation and Advanced Materials, University Center of Nour Bachir, El Bayadh, Algeria

² Electrotechnical Engineering Laboratory, University of Saida, Saida, Algeria

ARTICLE INFO

Article Type:

Selected Article [©]

Article History:

Received: 26 October 2022

Revised: 18 December 2022

Accepted: 28 December 2022

Published: 31 December 2022

Editor of the Article:

M. E. Şahin

Keywords:

DTC, PMSM, Fuzzy logic, Artificial intelligence

ABSTRACT

To satisfy the requirements of electric traction, the direct torque control (DTC) strategy for permanent magnet synchronous motor (PMSM) drives is the best candidate for high performance control. However, high torque and flux ripples can be observed because of an included switching table, and there are some of its drawbacks. To achieve a fast and reliable torque response and overcome these limitations, the basic DTC strategy based on fuzzy logic control (FLC) which integrated a space vector pulse width modulation (SVPWM) algorithm is proposed. The modified scheme uses the stator flux and the torque errors through two fuzzy logic controllers to generate a voltage space vector to provide the inverter switching states. To support the research, theoretical development and simulation results using the conventional and enhanced DTC are provided and compared.

Cite this article: A. E. Rabhi, K. Hartani, Y. Guettaf, "Direct torque control improvement for PMSM drive based on FLC," *Turkish Journal of Electromechanics & Energy*, 7(3), pp.120-126, 2022.

1. INTRODUCTION

These traction motors used in electric vehicles typically need frequent starts, stops, rapid acceleration, rapid deceleration, high torque low-speed hill climbing, and low torque and high-speed cruising. Furthermore, the traction motors must possess two crucial qualities: a low torque ripple that must not exceed 2% to prevent uncomfortable mechanical vibrations and vehicle noise, and a fast and robust torque response that is required in a wide speed range to meet the driver's instantaneous torque demand. Nowadays, PMSMs are expected to be applied to propulsion systems of electric vehicles for their high power and torque density, high efficiency, large constant power operation region, robust mechanical construction, and cost-effectiveness. However, their large torque ripple is an obstacle in the practical applications of PMSMs. The torque ripple reduction of PMSM for vehicle traction applications has also received great attention because large torque ripple can create uncomfortable vibrations and mechanical damage and even lead to vehicle instability.

The direct torque control (DTC) was proposed by Takahashi [1] in the mid-1980s, and it is known as an effective technique of control in a wide variety of electric power systems [2].

Recently, the DTC scheme for PMSM drives has received enormous attention in industrial motor drive applications due to its potential advantages and practicality in embedded systems. Unluckily, the major drawback of DTC is the high torque ripple,

which is due to the presence of hysteresis controllers and the limited number of available voltage vectors.

Several academic studies have been realized to improve this classical control method by integrating new techniques; such as artificial intelligence (AI) more developed in the last decades [3-6, 8-9].

In 1997, a study on fuzzy logic control (FLC) with DTC have been proposed [3], and the artificial neural network (ANN) was also proposed in 2001 by using Neural Networks in DTC of a three-level inverter [4]. These two approaches to intelligent techniques applied for induction motors have been compared with conventional DTC in 2007 [5].

Recently between 2011 and 2021, the studies [6-10] have remarkably reduced the torque ripples by using an adaptive FLC [11] or by using ANN based on a DTC PMSM drive.

This paper describes the conventional DTC blocs with the three-level inverter and the PMSM motor model in section two. The proposed FL-DTC is developed with space vector pulse with modulation SVPWM algorithm in section three. Section four is dedicated to the simulation and summarizes the results and the discussion of compiled previous studies for AI-DTC and the comparison of DTC with the proposed FL-DTC. Finally, a general conclusion is drawn.

[©] Initial version of this paper was selected from the proceedings of International Conference on Advanced Engineering Technologies (ICADET 2022) which was held on September 28-30, 2022, in Bayburt, TURKEY; and was subjected to peer-review process before its publication.

*Corresponding author's e-mail: rabhi31000@yahoo.fr

2. PRINCIPAL OF THE DIRECT TORQUE CONTROL

Its principle is to control directly the torque and stator flux of the motor, it includes two estimators, two hysteresis controllers, and a switching table. In our case, this control is applied for a PMSM, powered by the 3-level Inverter, and proportional-integral (PI) regulator to control the motor speed. The scheme is presented in Figure 1.

2.1. Modeling of the PMSM

The PMSM electric circuit equations with Concordia's transformation, based on Faraday's law, can be written as follows:

$$\begin{cases} V_{s\alpha} = R_s i_{s\alpha} + \frac{d\Phi_{s\alpha}}{dt} \\ V_{s\beta} = R_s i_{s\beta} + \frac{d\Phi_{s\beta}}{dt} \end{cases} \quad (1)$$

where $\Phi_{s\alpha}$ and $\Phi_{s\beta}$ are the α, β -axis flux linkage, which can be defined as follows:

$$\begin{cases} \Phi_{s\alpha} = L_s i_{s\alpha} + \Phi_f \cos\theta \\ \Phi_{s\beta} = L_s i_{s\beta} + \Phi_f \sin\theta \end{cases} \quad (2)$$

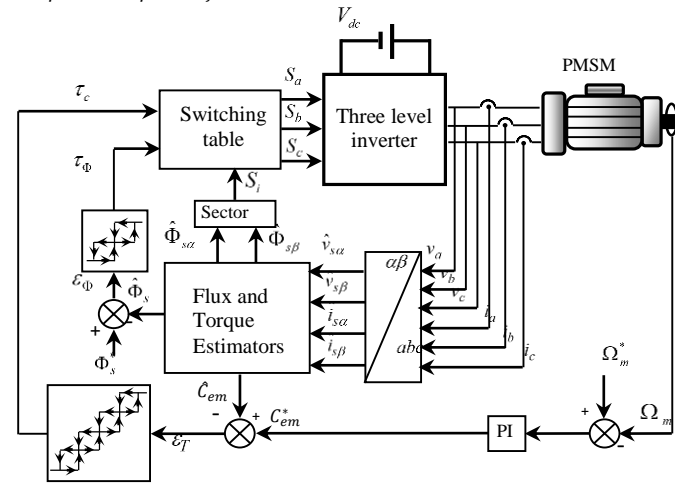


Fig. 1. Block diagram of the direct torque controller.

The motor's dynamic equations can be written as follows:

- Mechanical equation:

$$J \frac{d\omega_m}{dt} + C_f = C_{em} - C_r \quad (3)$$

- Stator flux and torque estimation:

The amplitude of stator flux and position θ_{ϕ_s} can be estimated by:

$$\begin{cases} \Phi_s = \sqrt{\Phi_{s\alpha}^2 + \Phi_{s\beta}^2} \\ \theta_{\phi_s} = \tan^{-1} \left(\frac{\Phi_{s\beta}}{\Phi_{s\alpha}} \right) \end{cases} \quad (4)$$

Where:

$$\begin{cases} \Phi_{s\alpha} = \int_0^t (v_{s\alpha} - R_s i_{s\alpha}) dt \\ \Phi_{s\beta} = \int_0^t (v_{s\beta} - R_s i_{s\beta}) dt \end{cases} \quad (5)$$

Figure 2 represents the different position possibilities of the position θ_{ϕ_s} , over a 2π interval, in the case of subdivision into 12 sectors.

The developed output torque expression can be estimated by:

$$C_{em} = \frac{3}{2} P (\Phi_{s\alpha} i_{s\beta} - \Phi_{s\beta} i_{s\alpha}) \quad (6)$$

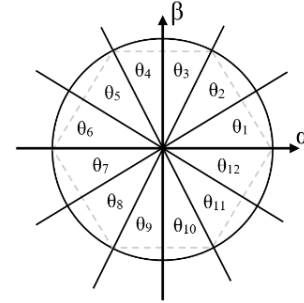


Fig. 2. Sectors subdivision.

2.2. Hysteresis Controllers

The 3-level hysteresis comparators are used to control the stator flux. The value of the output signal τ_ϕ is depending on the error ε_ϕ as follows in Equation (7):

$$\begin{cases} \varepsilon_\phi < \Delta_\phi \\ -\Delta_\phi < \varepsilon_\phi < \Delta_\phi \\ \varepsilon_\phi > \Delta_\phi \end{cases} \rightarrow \begin{cases} \tau_\phi = +1 \\ \tau_\phi = 0 \\ \tau_\phi = -1 \end{cases} \quad (7)$$

And a 5-level for the torque with two upper bands ($\Delta C_{max1}, \Delta C_{max2}$) and two lower bands ($\Delta C_{min1}, \Delta C_{min2}$). The value of the output signal τ_c is depending on the error ε_c as follows in Equation (8):

$$\begin{cases} \varepsilon_c < \Delta C_{min2} \\ \Delta C_{min2} \leq \varepsilon_c \leq \Delta C_{min1} \\ \Delta C_{min1} \leq \varepsilon_c \leq \Delta C_{max1} \\ \Delta C_{min1} \leq \varepsilon_c \leq \Delta C_{max2} \\ \varepsilon_c > \Delta C_{max2} \end{cases} \rightarrow \begin{cases} \tau_c = +2 \\ \tau_c = +1 \\ \tau_c = 0 \\ \tau_c = -1 \\ \tau_c = -2 \end{cases} \quad (8)$$

2.3. Switching Table

To provide the necessary commands to increase or decrease the flux and the torque, a switching table Table 1 is employed to determine the correct voltage vector, depending on the sector number (from 1 to 12) and on the signals produced by the two-hysteresis controller.

Table 1. Switching table of PMSM DTC 3-Level NPC inverter.

τ_ϕ	τ_c	Stator Flux Sector											
		1	2	3	4	5	6	7	8	9	10	11	12
+1	+2	\vec{V}_2	\vec{V}_3	\vec{V}_4	\vec{V}_5	\vec{V}_6	\vec{V}_7	\vec{V}_8	\vec{V}_9	\vec{V}_{10}	\vec{V}_{11}	\vec{V}_{12}	\vec{V}_1
	+1	\vec{V}_2	\vec{V}_{15}	\vec{V}_4	\vec{V}_{17}	\vec{V}_6	\vec{V}_{19}	\vec{V}_8	\vec{V}_{21}	\vec{V}_{10}	\vec{V}_{23}	\vec{V}_{12}	\vec{V}_{13}
	0	\vec{V}_{25}	\vec{V}_{26}	\vec{V}_{27}	\vec{V}_{25}	\vec{V}_{26}	\vec{V}_{27}	\vec{V}_{25}	\vec{V}_{26}	\vec{V}_{27}	\vec{V}_{25}	\vec{V}_{26}	\vec{V}_{27}
	-1	\vec{V}_{12}	\vec{V}_{13}	\vec{V}_2	\vec{V}_{15}	\vec{V}_4	\vec{V}_{17}	\vec{V}_6	\vec{V}_{19}	\vec{V}_8	\vec{V}_{21}	\vec{V}_{10}	\vec{V}_{23}
	-2	\vec{V}_{12}	\vec{V}_1	\vec{V}_2	\vec{V}_3	\vec{V}_4	\vec{V}_5	\vec{V}_6	\vec{V}_7	\vec{V}_8	\vec{V}_9	\vec{V}_{10}	\vec{V}_{11}
0	+2	\vec{V}_4	\vec{V}_5	\vec{V}_6	\vec{V}_7	\vec{V}_8	\vec{V}_9	\vec{V}_{10}	\vec{V}_{11}	\vec{V}_{12}	\vec{V}_1	\vec{V}_2	\vec{V}_3
	+1	\vec{V}_4	\vec{V}_{17}	\vec{V}_6	\vec{V}_{19}	\vec{V}_8	\vec{V}_9	\vec{V}_{10}	\vec{V}_{11}	\vec{V}_{12}	\vec{V}_1	\vec{V}_2	\vec{V}_3
	0	\vec{V}_{25}	\vec{V}_{26}	\vec{V}_{27}	\vec{V}_{25}	\vec{V}_{26}	\vec{V}_{27}	\vec{V}_{25}	\vec{V}_{26}	\vec{V}_{27}	\vec{V}_{25}	\vec{V}_{26}	\vec{V}_{27}
	-1	\vec{V}_{10}	\vec{V}_{23}	\vec{V}_{12}	\vec{V}_{13}	\vec{V}_2	\vec{V}_{15}	\vec{V}_{10}	\vec{V}_{17}	\vec{V}_6	\vec{V}_{19}	\vec{V}_8	\vec{V}_{21}
	-2	\vec{V}_{10}	\vec{V}_{11}	\vec{V}_{12}	\vec{V}_1	\vec{V}_2	\vec{V}_3	\vec{V}_4	\vec{V}_5	\vec{V}_6	\vec{V}_7	\vec{V}_8	\vec{V}_9
-1	+2	\vec{V}_5	\vec{V}_6	\vec{V}_7	\vec{V}_8	\vec{V}_9	\vec{V}_{10}	\vec{V}_{11}	\vec{V}_{12}	\vec{V}_1	\vec{V}_2	\vec{V}_3	\vec{V}_4
	+1	\vec{V}_{17}	\vec{V}_6	\vec{V}_{19}	\vec{V}_8	\vec{V}_{21}	\vec{V}_{10}	\vec{V}_{23}	\vec{V}_{12}	\vec{V}_{13}	\vec{V}_2	\vec{V}_{15}	\vec{V}_4
	0	\vec{V}_{25}	\vec{V}_{26}	\vec{V}_{27}	\vec{V}_{25}	\vec{V}_{26}	\vec{V}_{27}	\vec{V}_{25}	\vec{V}_{26}	\vec{V}_{27}	\vec{V}_{25}	\vec{V}_{26}	\vec{V}_{27}
	-1	\vec{V}_{21}	\vec{V}_{10}	\vec{V}_{23}	\vec{V}_{12}	\vec{V}_{13}	\vec{V}_2	\vec{V}_{15}	\vec{V}_4	\vec{V}_{17}	\vec{V}_6	\vec{V}_{19}	\vec{V}_8
	-2	\vec{V}_9	\vec{V}_{10}	\vec{V}_{11}	\vec{V}_{12}	\vec{V}_1	\vec{V}_2	\vec{V}_3	\vec{V}_4	\vec{V}_5	\vec{V}_6	\vec{V}_7	\vec{V}_8

2.4. Speed Regulator

To keep the speed constant, a proportional integral PI regulator is inserted into the speed loop as shown in Figure 3, which enables the reference torque to be determined.

The relationship between the speed and the electromagnetic torque is given by the open-loop transfer function of Equation (9):

$$F(s) = \frac{k_m}{1 + \tau_m s} \quad (9)$$

where, $k_m = (P/f)$ and $\tau_m = (J/f)$. P : pole pairs number J : the moment of inertia and f_c : friction coefficient. C_r : resistive torque. The k_i and k_p are the integral and proportional gains of the regulator are thus obtained:

$$\begin{cases} k_p = \frac{2\zeta\omega_N\tau_m^{-1}}{k_m} \\ k_i = \frac{\omega_N^2\tau_m}{k_mk_p} \end{cases} \quad (10)$$

where ζ is the damping ratio of the system and ω_N is the undamped natural frequency of the control loop.

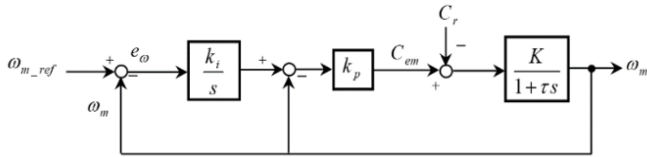


Fig. 3. Block diagram of the PI speed regulator.

2.5. Three-level Inverter

The model of the inverter as shown in Figure 4 can be represented as follows:

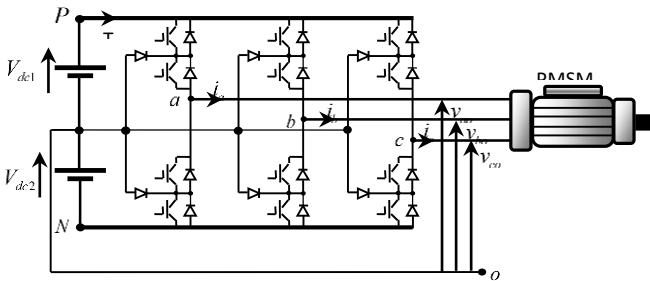


Fig. 4. Three-level-inverter diagram.

$$\begin{bmatrix} V_a \\ V_b \\ V_c \end{bmatrix} = \frac{1}{6} \begin{bmatrix} 2 & -1 & -1 \\ -1 & 2 & -1 \\ -1 & -1 & 2 \end{bmatrix} \begin{bmatrix} F_{11}^b - F_{10}^b \\ F_{21}^b - F_{20}^b \\ F_{31}^b - F_{30}^b \end{bmatrix} V_{dc} \quad (11)$$

The T switch connection function is $F=1/0$, and the switching state of the three arms is simplified by the following relation:

$$\begin{bmatrix} S_a \\ S_b \\ S_c \end{bmatrix} = \begin{bmatrix} F_{11}^b - F_{10}^b \\ F_{21}^b - F_{20}^b \\ F_{31}^b - F_{30}^b \end{bmatrix} \quad (12)$$

where: $S_x = F_{i1}^b - F_{i0}^b$, $x=a, b, c$, $i=1, 2, 3$.

3. DTC BASED ON FUZZY LOGIC CONTROL

To improve the performances of the conventional DTC, the flux and torque hysteresis controllers and the switching table are replaced by a fuzzy logic controller in Figure 5.

With the conventional DTC, it is not possible to keep the stator flux amplitude constant, since only two vectors of fixed voltages allow the stator flux to remain around its reference value during the duration of each sector of the hexagon as seen in Figure 6.

In addition, the amplitude of the voltage vector always takes the maximum value, which leads to important variations in the flux's position and the value of the torque [13]. Therefore, strong ripples will be generated.

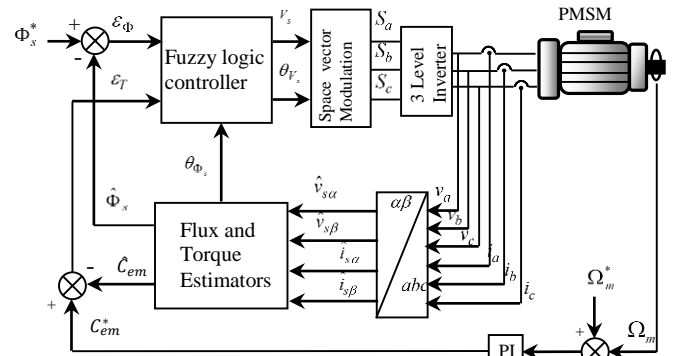


Fig. 5. Block diagram of the direct torque fuzzy controller.

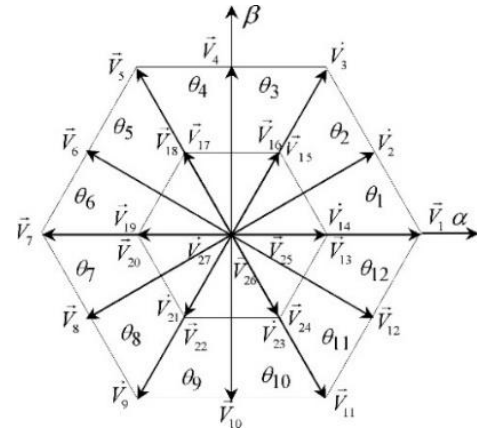


Fig. 6. Vector diagram of a three-phase three-level inverter.

To approach the reference values for the flux and the torque, fuzzy logic generates the angle and the voltage vectors, which are then used by SVPWM to control the state of the 3-level inverter switches.

3.1. Fuzzy Logic Controllers Conception

The torque and the stator flux errors are used as the two (02) inputs of the FLC as shown in Figure 8, which consist of two types of fuzzy controllers (FLC1 and FLC2).

- *The FLC1*: To select voltage vector position:

It is the Sugeno type, and the position of the voltage vector is chosen to keep the flux and the torque around their reference value according to their standard errors the values of the angle δ is chosen, which are summarized in Table 2.

Table 2. Selected angle δ .

ε_{ϕ}^n	P			Z			N		
ε_c^n	P	Z	N	P	Z	N	P	Z	N
δ	$\frac{\pi}{4}$	0	$-\frac{\pi}{4}$	$\frac{\pi}{2}$	$\frac{\pi}{2}$	$-\frac{\pi}{2}$	$\frac{3\pi}{4}$	π	$-\frac{3\pi}{4}$

The input variables are chosen for the normalized flux error in the range [-0.1, 0.1] and in the range [-1, 1] for the normalized torque error, represented respectively by Figure 7 (a, b), with triangular and trapezoidal membership functions.

• *The FLC2*: To select the voltage vector magnitude:

It is a Mamdani type, designed to select the modulus of the voltage vector, to minimize flux and torque errors.

With the same method as FLC1, the triangular and the trapezoidal membership functions were chosen for the input and output variables of the controller in the range [-0.1, 0.1] for the normalized flux error, [-1, 1] for the normalized torque error, respectively, by Figure 8. Table 3 summarizes the fuzzy rules.

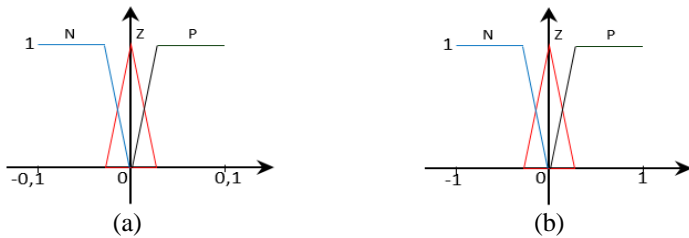


Fig. 7. Membership functions for the FLC1, (a) flux error, (b) torque error.

Table 3. Fuzzy rules table FLC2.

\tilde{u}_{V_s}	\tilde{e}_c						
	NG	NM	NP	EZ	PP	PM	PG
\tilde{e}_{ϕ}	NG	PG	PM	PP	PP	PM	PG
	NM	PG	PM	PP	PP	PM	PG
	NP	PG	PM	PP	EZ	PP	PM
	EZ	PG	PM	PP	EZ	PP	PM
	PP	PG	PM	PP	EZ	PP	PM
	PM	PG	PM	PP	PP	PP	PM
	PG	PG	PM	PP	PP	PP	PM

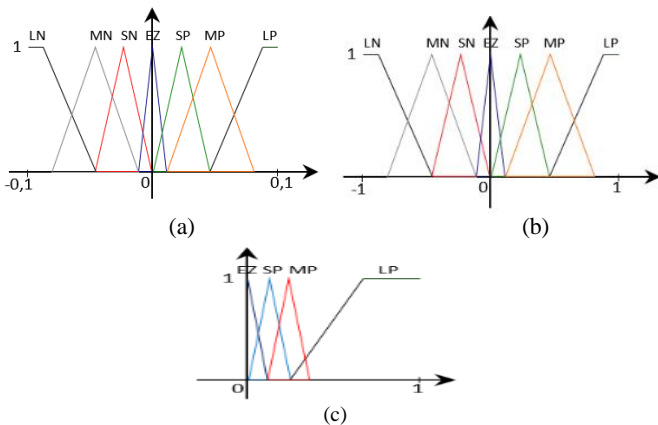


Fig. 8. Membership functions for the FLC2, (a) flux error (b) torque error (c) reference voltage.

3. 2. Three-Level SVPWM Algorithm

The three-level inverter can generate 27 vectors by switching states $S_a, S_b,$ and $S_c,$ which can be divided into four groups as shown in Figure 6, in the first sector ($0 < \theta < \pi/3$): (V_0) is the zero voltage vector, (V_{13} and V_{15}) are the small voltage vectors, (V_2) is the middle voltage vector and (V_1 and V_2) are the large voltage vectors.

Identically to the two-level SVPWM [12], the sector is divided into four regions as seen in Figure 9 to select three adjacent voltage vectors $V_{r1}, V_{r2},$ and $V_{r3}.$

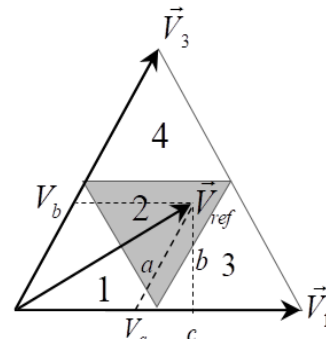


Fig. 9. The reference voltage vector's belonging region.

3.3. Three-Level SVPWM Algorithm

Depending on the reference voltage vector V_{ref} (angle and amplitude) three adjacent voltage vectors $V_{r1}, V_{r2},$ and V_{r3} are selected. The duration of each voltage vector can be obtained by the time averaging principle as follows Equation [12]:

$$V_{ref} T_s = V_{r1} t_1 + V_{r2} t_2 + V_{r3} t_3 \tag{13}$$

where T_s is the sampling time $T_s = t_1 + t_2 + t_3.$

The region of the reference voltage vector can be identified by the following algorithm [12]:

- if $V_a < \frac{V_{dc}}{3}$ & $V_b < \frac{V_{dc}}{3}$ & $V_a + V_b < \frac{V_{dc}}{3} \rightarrow \vec{V}_s$: Region 1
- if $V_a < \frac{V_{dc}}{3}$ & $V_b < \frac{V_{dc}}{3}$ & $V_a + V_b > \frac{V_{dc}}{3} \rightarrow \vec{V}_s$: Region 2
- if $V_a > \frac{V_{dc}}{3} \rightarrow \vec{V}_s$: Region 3
- if $V_b > \frac{V_{dc}}{3} \rightarrow \vec{V}_s$: Region 4

The selected voltage vectors for all sectors corresponding to the adjacent voltage vectors $V_{r1}, V_{r2},$ and V_{r3} are summarized in Table 4.

4. SIMULATION RESULTS AND DISCUSSION

The mathematical models of all blocks (PMSM, inverter, hysteresis controllers...) of conventional DTC, fuzzy logic controllers (FLC1, FLC2), and the SVPWM 3-level algorithms were established by MATLAB/Simulink software as shown in Figure 10 to simulate the same conditions and using the same parameters summarized in Table 5.

To make a comparison, we started with conventional - DTC simulation followed by FL-DTC simulation.

For the starting process, 600 rpm was set as a motor speed reference, and 40 N.m as a nominal load, a step torque load C_r of 20 N.m was applied at 0.8 seconds and removed at 1.4 seconds.

Table 4. Relations between the adjacent voltage vectors and the selected voltage vectors in all sectors.

Region	Sector 1			Sector 2			Sector 3			Sector 4			Sector 5			Sector 6		
	V_{r1}	V_{r2}	V_{r3}															
1	V_0	V_1	V_2	V_0	V_2	V_3	V_0	V_3	V_4	V_0	V_4	V_5	V_0	V_5	V_6	V_0	V_6	V_1
2	V_1	V_{15}	V_{21}	V_2	V_{16}	V_{22}	V_3	V_{17}	V_{23}	V_4	V_{18}	V_{24}	V_5	V_{19}	V_{25}	V_6	V_{20}	V_{26}
3	V_1	V_{21}	V_2	V_2	V_{22}	V_3	V_3	V_{23}	V_4	V_4	V_{24}	V_5	V_5	V_{25}	V_6	V_6	V_{26}	V_1
4	V_2	V_{16}	V_{21}	V_3	V_{17}	V_{22}	V_4	V_{18}	V_{23}	V_5	V_{19}	V_{24}	V_6	V_{20}	V_{25}	V_1	V_{15}	V_{26}

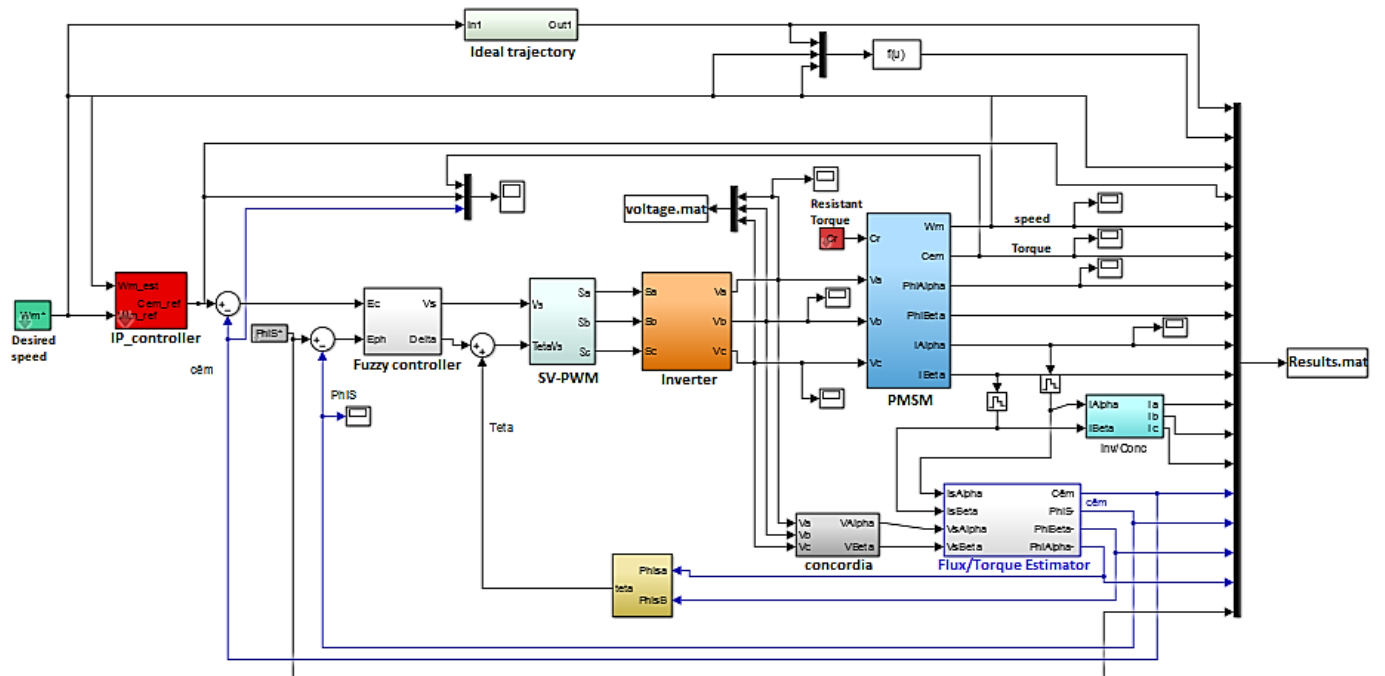


Fig. 10. The reference voltage vector's belonging region.

Table 5. Simulation parameters.

Symbol	Parameter	Value
P_e	Nominal power	30 kW
T_m	Maximal torque	145 Nm
V_s	Line to line voltage	230 V
R_s	Stator resistance	0.03 Ω
L_d	Stator inductance	0.2 mH
Φ_f	Permanent magnet flux linkage	0.08 Wb
p	Number of pole pairs	4
K_i	Integral gain	25
K_p	Proportional gain	0.775
G_{Phi}	FLC gain flux	30
G_{Cem}	FLC gain torque	8

To compare the conventional-DTC and FL-DTC, the results of these two methods were merged into the same curves to ease the comparison and are summarized in Table 6. The first simulated parameters are the speed curves illustrated in Figure 11.

We notice the same pace for the two methods which follow the reference value of 600 rpm, due to the PI regulator, which also offers robustness against the applied load. With FL-DTC we observe an improvement in the rise time response, its value is indicated in Table 6.

The torque and the flux are the two most important parameters, in the curves illustrated respectively in Figure 12 and Figure 13. Noticed that the ripples of these two parameters are effectively reduced, with the FL-DTC, especially for the torque. These values are also shown in Table 6.

Table 6. Comparative simulation results.

Parameters	Conventional DTC	Fuzzy DTC
Max torque ripple	7.04	3.58
Max flux ripple	0.0012	0.0011
Rise time at 5%	0.097	0.094

In addition, the results of some previous studies compiled in Table 7 prove the improvement of the DTC-PMSM by the introduction of additional techniques such as; ANN, FL.

Table 7. Previous studies results.

Method	ANN-Based DTC Driver for PMSM [6]	Fuzzy DTC of PMSM based on space vector modulation(SVM) [7]	DTC Based on ANN of a Five-Phase PMSM Drive [8]	DTC based on Adaptive FL Control and Optimization of a PMSM [11]
Results	<ul style="list-style-type: none"> A torque ripples are reducing remarkably in a steady state. 	<ul style="list-style-type: none"> A reduction of the Torque and flux ripples. A reduction of the switching losses (in the inverter and harmonics). 	<ul style="list-style-type: none"> Torque ripples are significantly reduced in a steady state. Fast and better response. 	<ul style="list-style-type: none"> A reduction of the Torque ripples. High: dynamic response. A reduction of the switching frequency.

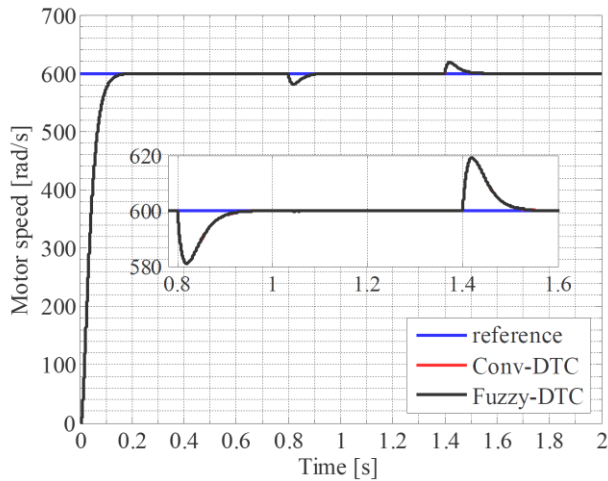


Fig. 11. Motor speed.

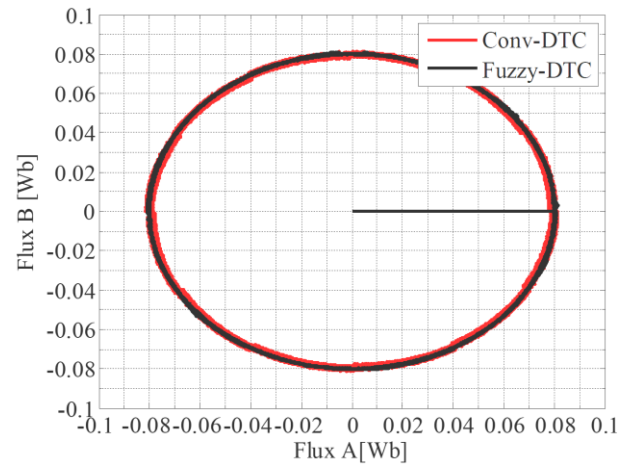


Fig. 13. Stator flux trajectory.

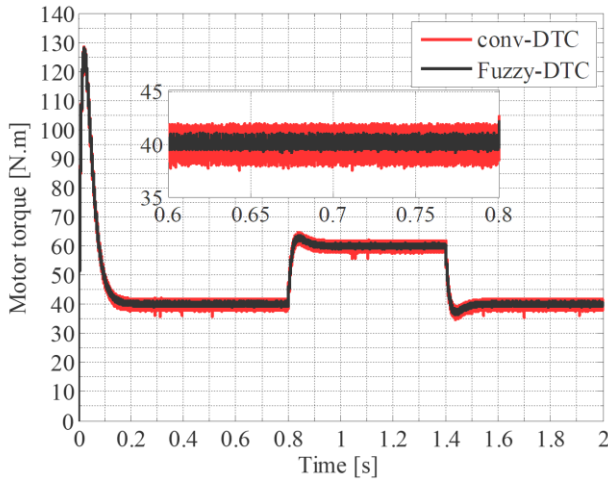


Fig. 12. Electromagnetic torque response.

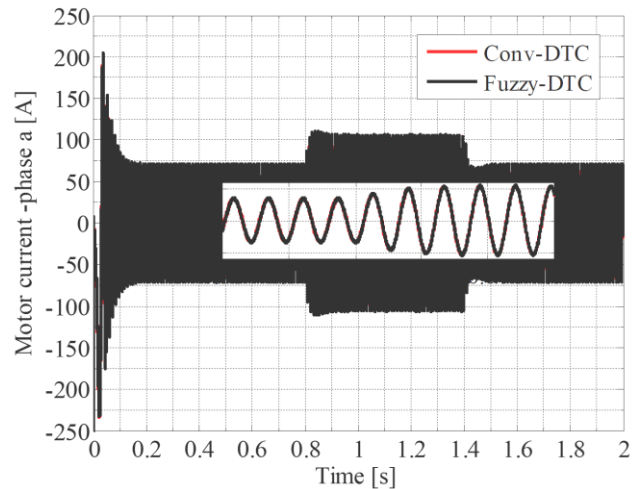


Fig. 14. Stator's current response.

5. CONCLUSION

The research proposes a new fuzzy logic control FLC technique based on space vector pulse width modulation SVPWM algorithm for permanent magnet synchronous motor PMSM to enhance the dynamic performance of direct torque control DTC and reduce torque ripple. The suggested DTC technique generates a voltage space vector by operating on both the amplitude and the angle of its components to generate the inverter switching states. It does this by using the stator flux amplitude and the electromagnetic torque errors through two fuzzy logic controllers. Simulated comparisons with conventional DTC have been developed. The results demonstrated that the suggested DTC

minimizes torque and flux ripples while maintaining a robust dynamic torque response, which is a characteristic of DTC performance.

References

[1] I. Takahashi and Y. Ohmori, "High-performance direct torque control of an induction motor," *IEEE Transactions on Industry Applications*, 25(2), pp. 257-264, 1989.
 [2] Z. Mokrani, D. Rekioua, T. Rekioua, "Control of fuel cells-electric vehicle based on direct torque control," *Turkish Journal of Electromechanics & Energy*, 3(2), pp. 8-14, 2018.

[3] Y. Xia, and W. Oghanna, "Study on fuzzy control of induction machine with direct torque control approach," *ISIE '97 Proceeding of the IEEE International Symposium on Industrial Electronics*, vol. 2, pp.625-630, 1997.

[4] X. Wu, and L. Huang, "Direct torque control of three-level inverter using neural networks as switching vector selector," *Conference Record of the 2001 IEEE Industry Applications Conference, 36th IAS Annual Meeting (Cat. No.01CH37248)*, vol. 2, pp. 939-944, 2001.

[5] R. Toufouti, S.Meziane, H. Benalla, "Direct torque control for induction motor using intelligent techniques," *Journal of Theoretical & Applied Information Technology*, 3(3), pp. 35-44, 2007.

[6] F. Korkmaz, M. F. Cakır, İ. Topaloğlu, R.Gurbuz, "Artificial Neural Network Based DTC Driver for PMSM," *International Journal of Instrumentation and Control Systems (IJICS)*, 3(1), pp.1-7, 2013.

[7] O. Ouledaliab A.Meroufelb P.Wiraab S.Bentoubaab "Direct Torque Fuzzy Control of PMSM based on SVM," *University of Adrar Algeria, Energy Procedia* 74, pp. 1314-1322, 2015.

[8] T. Kamel, D. Abdelkader, B. Said, A. Iqbal, "Direct torque control based on artificial neural network of a five-phase PMSM drive," *In Hatti M. (eds) Artificial Intelligence in Renewable Energetic Systems. ICAIRES 2017*.

[9] M. Guiti, A. Nait seghir "Direct Torque Control with ANN hysteresis controller for PMSM" *USTHB, ALGERIA 2015 4th International Conference on Electrical Engineering (ICEE)*, pp. 1-6, 2015.

[10] N. Henini, A. Tlemcani, S. Barkat, "Adaptive Interval Type-2 Fuzzy Controller Based Direct Torque Control of Permanent Magnet Synchronous Motor," *Advances in Electrical and Computer Engineering*, 21(2), pp.15-22, 2021.

[11] H. Mesloub, M. T. Benchouia, R. Boumaaraf, A. Golea, N. Golea, M. Becherif, "Design and implementation of DTC based on AFLC and PSO of a PMSM," *Mathematics and Computers in Simulation*, vol. 167, pp. 340-355, 2020.

[12] A. K. Gupta, and A. M. Khambadkone "A space vector PWM scheme for multilevel inverters based on two-level space vector PWM," *IEEE Transactions on industrial electronics*, vol. 53, pp. 1631-1639, 2006.

[13] B.-R. Lin, "Analysis and implementation of a three-level PWM rectifier/inverter," *IEEE Transactions on Aerospace and electronic systems*, vol. 36, pp. 948-956, 2000.

[14] K. Hartani, Y. Miloud, and A. Miloudi, "Improved direct torque control of permanent magnet synchronous electrical vehicle motor with proportional-integral resistance estimator," *Journal of Electrical Engineering and Technology*, vol. 5, pp. 451-461, 2010.

Biographies

Abderrahmane Eldjallil Rabhi was born in Algeria. He is an electrical engineer and researcher. He is also a member of the Instrumentation and Advanced Materials Laboratory (LIMA) at the University Center Nour Bachir El Bayadh, Algeria. His research interests involve electrical systems, automation, control, estimation, and electric vehicle applications.

E-mail: rabhi31000@yahoo.fr



Hartani Kada is a lecturer in the Electrical & Engineering Department at the University of Saida, Algeria since 2003. He was born in Saida, Algeria in 1976. He obtained his Doctorate in Electrical Control from the University of Sciences and Technology (USTO), Oran, Algeria, in 2007; M.S. in electrical control from the University of Sciences and Technology (USTO), Oran, Algeria, 2003; B.S. in Electrotechnical Engineering from the University of Saida, Algeria, in 1997. Currently, he is a Professor in electrical control and director of the Electrotechnical Engineering Laboratory at the University of Saida, Algeria. His fields of interest include multi-machine multi-converter systems, antilock brake systems, traction control systems, and anti-skid control for electric vehicles.

E-mail: kada_hartani@yahoo.fr



Yacine Guettaf was born in Tiaret, Algeria, in 1986. He received the magister and the Ph.D. degrees (with honors) respectively, in 2012 and 2016, from the University of Sciences and Technology of Oran (USTO MB), Algeria. The main focus of his research is power electronics devices and their integration into electrical energy management systems. He is currently the Director of the Research Laboratory: Instrumentation and Advanced Materials (LIMA) and a Teacher-Researcher at the University Center of El Bayadh, Algeria.

E-mail: y_guettaf@yahoo.fr